nature geoscience

ARTICLES

https://doi.org/10.1038/s41561-022-00893-7

Plate tectonic chain reaction revealed by noise in the Cretaceous quiet zone

Derya Gürer[1,3]✉, Roi Granot[2] and Douwe J. J. van Hinsbergen[1]

Global reorganizations of tectonic plates may be caused by a trigger such as a continental collision or a rising mantle plume. However, whether and how such a trigger propagates through a plate circuit remains unclear. Here we use a plate kinematic model to quantify relative motions between the African and Eurasian plates following a plume-induced plate motion change that triggered formation of a new subduction zone within the Neotethys Ocean at 105 Ma. We constrain the plate kinematic model by geomagnetic intensity variations recorded in Atlantic quiet zone crust that formed during the Cretaceous Normal Superchron (126–83 Ma), during which magnetic reversals were absent. We find that convergence rate changes between Africa and Eurasia are well explained by the initiation and arrest of the plume-induced subduction zone. Our plate kinematic model also reveals that the plate acceleration that followed upon subduction initiation changed the Africa–Eurasia convergence direction, which in turn was accommodated by subsequent subduction initiation about 85 Ma in the Alpine region that then triggered a cascade of regional tectonic events. This plate tectonic chain reaction illustrates how changes in plate motion, underpinned by mantle dynamics, may self-perpetuate through a plate circuit.

Pronounced changes in the velocity and/or direction of tectonic plate motions are short-lived events punctuating long periods of gradually evolving motion[1–3]. Inspection of global plate kinematic models and of geological records at plate boundaries have led to the hypothesis that plate motion changes are at times concentrated in 'global plate reorganizations': short-lived but ill-defined periods of ~10 Myr in which plate motions change across the globe. Such reorganizations, for example in the mid-Cretaceous, around 105 million years ago (Ma) (refs. [2–4]), or in the Eocene, around 50 Ma (refs. [5–8]), are suspected to be triggered by geodynamic coincidences such as rising mantle plumes[2], collisions[2–5] or ridge subduction[6–8]. However, to set off a global plate reorganization, plate motion changes induced by such isolated dynamic triggers must be able to cascade to neighbouring plates, for which a mechanism has so far not been identified.

We hypothesize that when a trigger causes a plate motion change, this change may in turn trigger subsequent plate motion changes in what we conceptualize as a 'plate tectonic chain reaction'. Geodynamic analysis has long recognized that the main drivers of plate motion are the negative buoyancy of subducted lithosphere (slab pull) and occasional short-lived and subtle effects of spreading mantle plume heads below the lithosphere (plume push[9–11]). Formation of new, or the abandonment of pre-existing, plate boundaries (mid-ocean ridges or subduction zones), at times combined with the arrival of mantle plumes, are thus widely believed to form the dynamic underpinning of observed plate motion changes[7,9–15]. Initiation of subduction of a plate, either spontaneously[16] or forced (for example, by ridge subduction[7,17] or by arrest, relocation or reversal of subduction) will change where and on which plates slab pull is exerted[14]. The onset or cessation of a slab pull force after initiation or arrest of subduction is, in turn, a logical driver of plate acceleration or deceleration, respectively[7,13,14,17]. Hence, while initiation of a new subduction zone may respond to an initial trigger (for example, plume push[18,19]), such initiations may also be forced by (the dynamic processes underlying) cascading plate motion changes. Subduction initiation events may thus form the links making plate tectonic chain reactions possible.

Recently, the study of ophiolites in Oman and Anatolia revealed that the formation of an intra-oceanic subduction zone around 105 Ma was forced by far-field stress changes[18]. This subduction zone formed in the Neotethys Ocean in the modern eastern Mediterranean region and continued to the western Indian Ocean, where it transitioned into a spreading ridge between India and Madagascar[11]. Its formation is proposed to result from the push of the Morondava plume head (Fig. 1b), causing an India–Africa plate motion change at ~105 Ma (ref. [11]). By 96–92 Ma, this subduction zone developed sufficient slab pull to drive upper plate extension widely recorded in the age of the crust of supra-subduction-zone ophiolites from the Mediterranean region to Oman and Pakistan[18]. Because forced initiation and development of pronounced slab pull are separated by ~10 Myr, this provides the opportunity to separate the dynamic causes from the consequences of this subduction zone, making this the ideal test case to evaluate the plausibility of plate tectonic chain reactions. To identify potential causes of subduction initiation, we explore kinematic predictions of generic numerical models to evaluate whether this onset of slab pull may in turn have been a trigger of a subsequent plate motion change and whether this change caused another plate boundary reorganization, thus defining a chain reaction. To do this required overcoming a notorious problem: the absence of plate kinematic constraints during the Cretaceous Normal Superchron (CNS), the 126–83 Ma (ref. [20]) period without magnetic polarity reversals expressed in the oceanic Cretaceous quiet zone (CQZ) crust. Therefore, we calculated the first Africa–Eurasia kinematic plate model for the CNS using recently identified magnetic intensity variations on the Atlantic CQZs[21]. This paved the path to analyse the dynamic propagation of plate tectonic chain reaction, which may be part of the enigmatic Cretaceous plate reorganization.

[1]Department of Earth Sciences, Utrecht University, Utrecht, the Netherlands. [2]Department of Earth and Environmental Sciences, Ben-Gurion University of the Negev, Beer-Sheva, Israel. [3]Present address: Research School of Earth Sciences, Australian National University, Canberra, Australian Capital Territory, Australia. ✉e-mail: derya.guerer@anu.edu.au

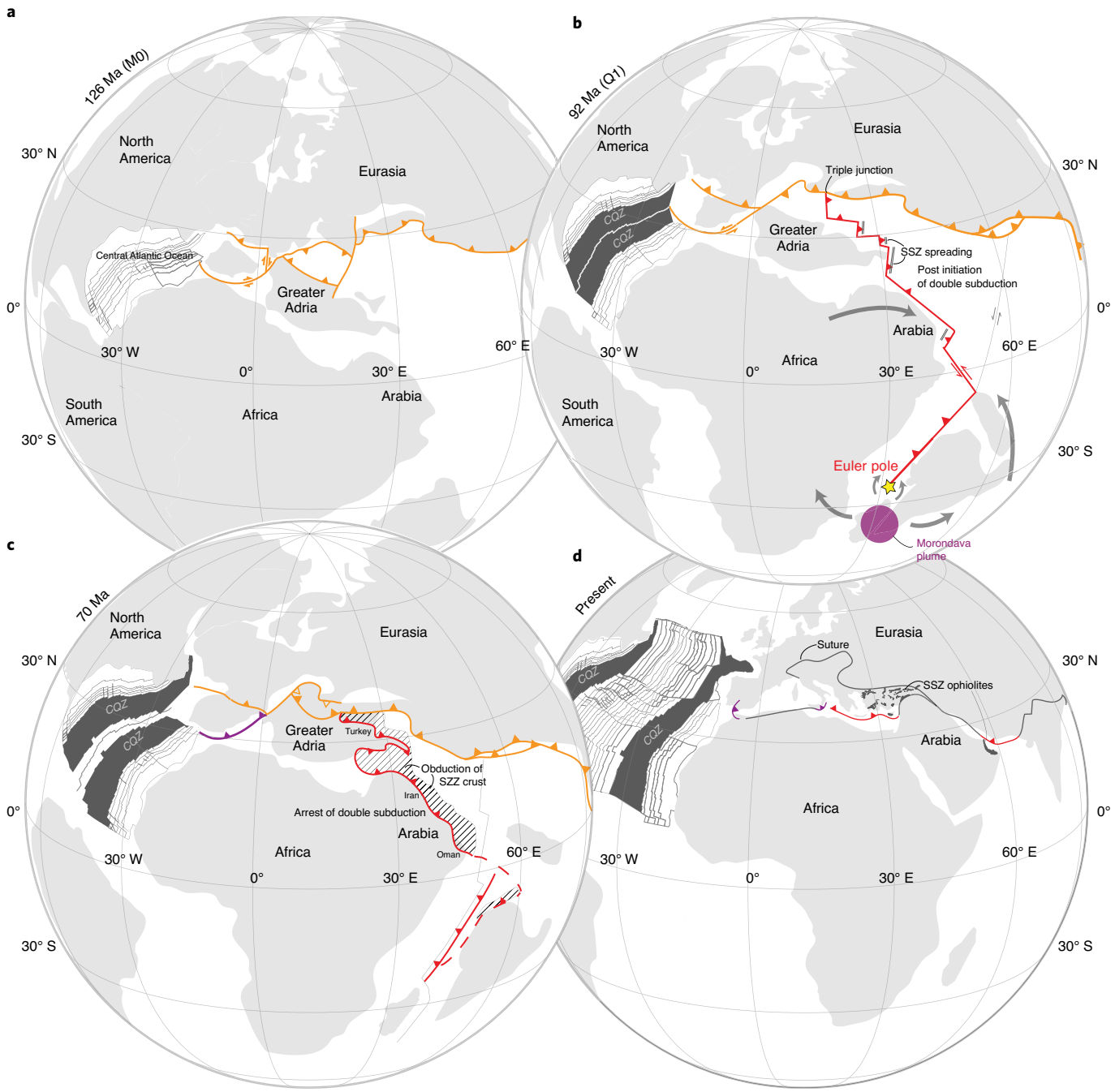

Fig. 1 | Plate boundary evolution of the Neotethys realm. a–c, We updated previous reconstructions[3] with Atlantic kinematic constraints at 126 Ma (corresponding to anomaly M0, the onset of the CNS) (**a**), 92 Ma (corresponding to Q1, following intra-Neotethyan subduction-zone initiation triggered by the arrival of the Morondava plume[11] and around the onset of pronounced slab pull) (**b**) and 70 Ma (corresponding to obduction of supra-subduction-zone (SSZ) crust (hatched) and arrest of the Neotethyan intra-oceanic subduction zone along Arabia and northeast Africa) and the formation of a new subduction zone in the western Mediterranean (purple) (**c**). **d**, Present-day configuration with distribution of Neotethyan ophiolites. Reconstructions portrayed in a slab-fitted mantle reference frame[46]. See Methods for details.

Global plate reorganizations and proposed triggers

The two most widely discussed global plate reorganizations are the Cretaceous (~105–100 Ma) (ref. [2]) and Eocene (~55–45 Ma) (ref. [5]) plate reorganizations. The Cretaceous reorganization, during the CNS, was inferred on the basis of changes in the Atlantic, Indian and northern Pacific fracture-zone orientations[2]. The age was loosely estimated on the basis of interpolation of seafloor spreading rates and further defined by inspection of tectonic events recorded in continental geological records across the globe in the 110–90 Ma period[2]. Tectonic shortening in western North America and East Asia, subduction along western South America, extension in Antarctica and Australia and basin instability in Africa and Europe were all used to identify this reorganization[2]. Proposed triggers include cessation of subduction along the east Australian–New Zealand margin due to collision of the Hikurangi ocean plateau[2], the rise of the Bouvet mantle plume in the South Atlantic Ocean[2],

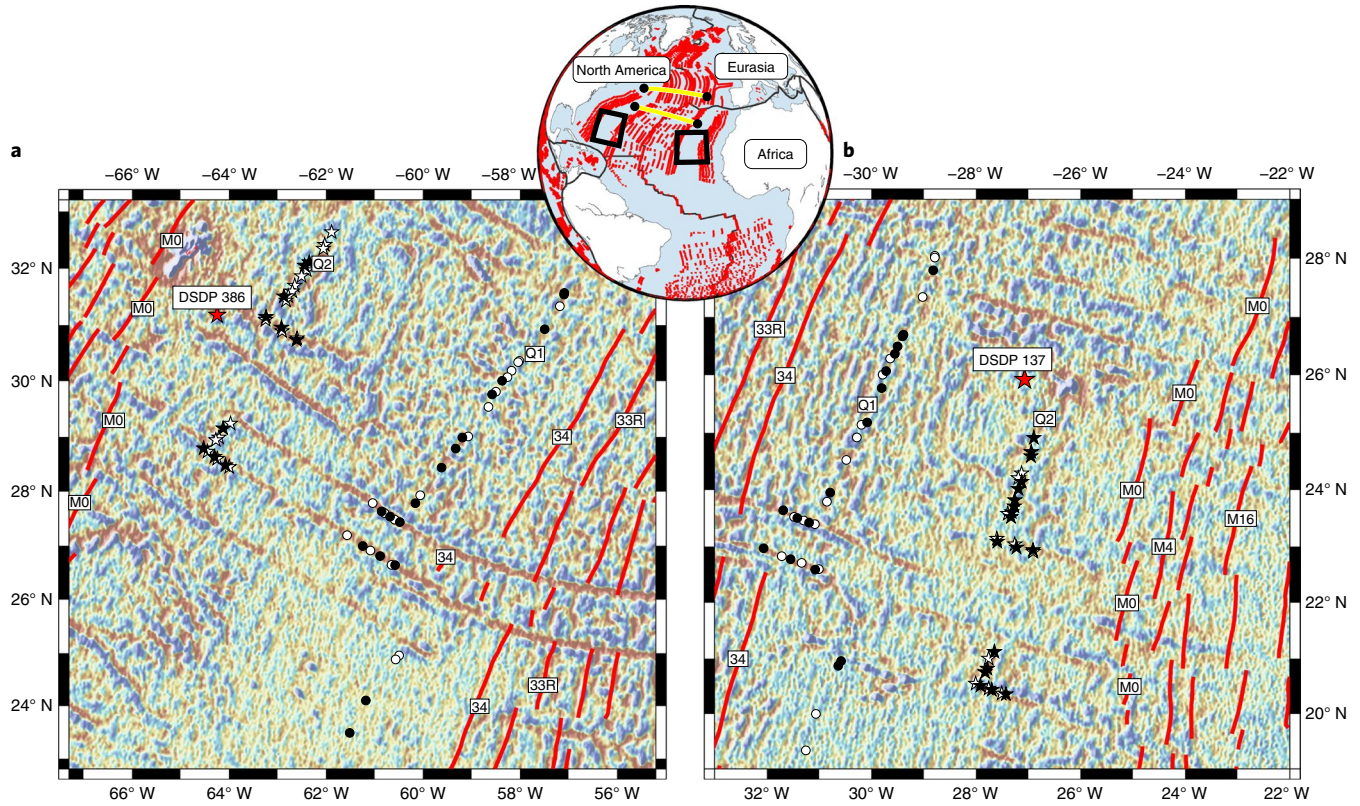

Fig. 2 | Noise in the quiet zone. Central Atlantic CQZ magnetic anomaly and fracture-zone picks that were used to compute CNS rotation pole parameters (Q1, circles; Q2, stars). **a**, North America. **b**, Africa. White and black symbols delineate the locations of the picks and reconstructed picks, respectively (wiggle plots are shown in Extended Data Fig. 1). Deep Sea Drilling Project (DSDP) drill-hole locations that were used to date Q1 and Q2[21] are marked by red stars. Background is the seafloor fabric as delineated by the vertical gravity gradient grids derived from satellite altimetry[47]. Note the curvature in fracture-zone orientations found towards the young end of the CQZ. Red lines mark locations of the reversals-related magnetic isochrons. Inset shows the Africa–North America–Eurasia plate circuit (yellow lines).

collision between microcontinents in Tibet[4] and the formation of an Andean-style subduction zone along continental Eurasia[3]. However, how these triggers would have propagated to cause changes ascribed to the reorganization remains undefined.

Similar to the Cretaceous reorganization, the Eocene plate reorganization is hypothesized on the basis of a series of plate kinematic changes across the globe, including the Pacific plate motion change reflected by the prominent change in the Hawaii–Emperor seamount chain, the formation of subduction zones, mid-ocean ridges, back-arc basins and orogens[5,8,22–26], yet it remains unclear whether this was the response to one single trigger or multiple unrelated triggers or how these kinematic changes dynamically propagated in space and time. Proposed drivers for all or part of the reorganization include initiation of Pacific Plate subduction (spontaneously[16] or by ridge subduction[7,8,17] or subduction polarity reversal[14]), collision of India and Asia[5], collisions and subduction relocation in western North America[27] and lower-mantle subduction of slabs below South America[28].

Intra-Neotethyan subduction initiation

We test our concept of a plate tectonic chain reaction through a case study of the initiation of a major intra-oceanic subduction zone in the Neotethys Ocean. During the mid-Cretaceous, an intra-oceanic subduction zone formed from a trench–trench–trench triple junction with a subduction zone that had already existed since Jurassic time along the southern Eurasian margin[19,22] to the west Indian Ocean, where the plate boundary transitioned into a rift (and later ridge) that ended in a ridge–ridge–ridge triple junction in the Southern Ocean[11]. This initiation of the intra-Neotethyan subduction zone generated a so-called double, in-line subduction-zone configuration between Africa and Eurasia and formed a new plate consisting predominantly of Neotethyan oceanic lithosphere[23] (Fig. 1b). In the latest Cretaceous, the southern rim of this plate was emplaced onto continental crust of Greater Adria, Africa and Arabia along the southern Neotethyan margin (black hatched area in Fig. 1c), and relics are today preserved as forearc supra-subduction-zone ophiolites in the eastern Mediterranean region and along northeastern Arabia and in mélanges in suture zones[22,24,25] (Fig. 1d). Geochemical and geochronological data show that the formation of oceanic crust of these ophiolites, due to upper plate extension and forearc spreading above a nascent subduction zone (so-called supra-subduction-zone ophiolites), began by ~96–95 Ma in Oman[24] and ~92 Ma in the eastern Mediterranean region[25]. These observations demonstrate that by this time, slab pull in the new subduction zone was sufficient to rupture the upper plate and must have exerted slab pull on the trailing African–Arabian plate[26,29]. The initiation of the subduction zone itself predated upper plate extension and was already under way by 104 Ma as constrained by garnet Lu/Hf geochronology of metamorphic soles below the Neotethyan ophiolites[18,30]. This temporal relationship demonstrates that convergence initiating subduction predated upper plate extension and must have been induced by a change in plate motion driven by far-field forcing[18]. Structural, geological and palaeomagnetic observations of metamorphic soles and supra-subduction ophiolitic crust suggest that incipient convergence was approximately east–west directed, highly oblique to the southern Neotethyan

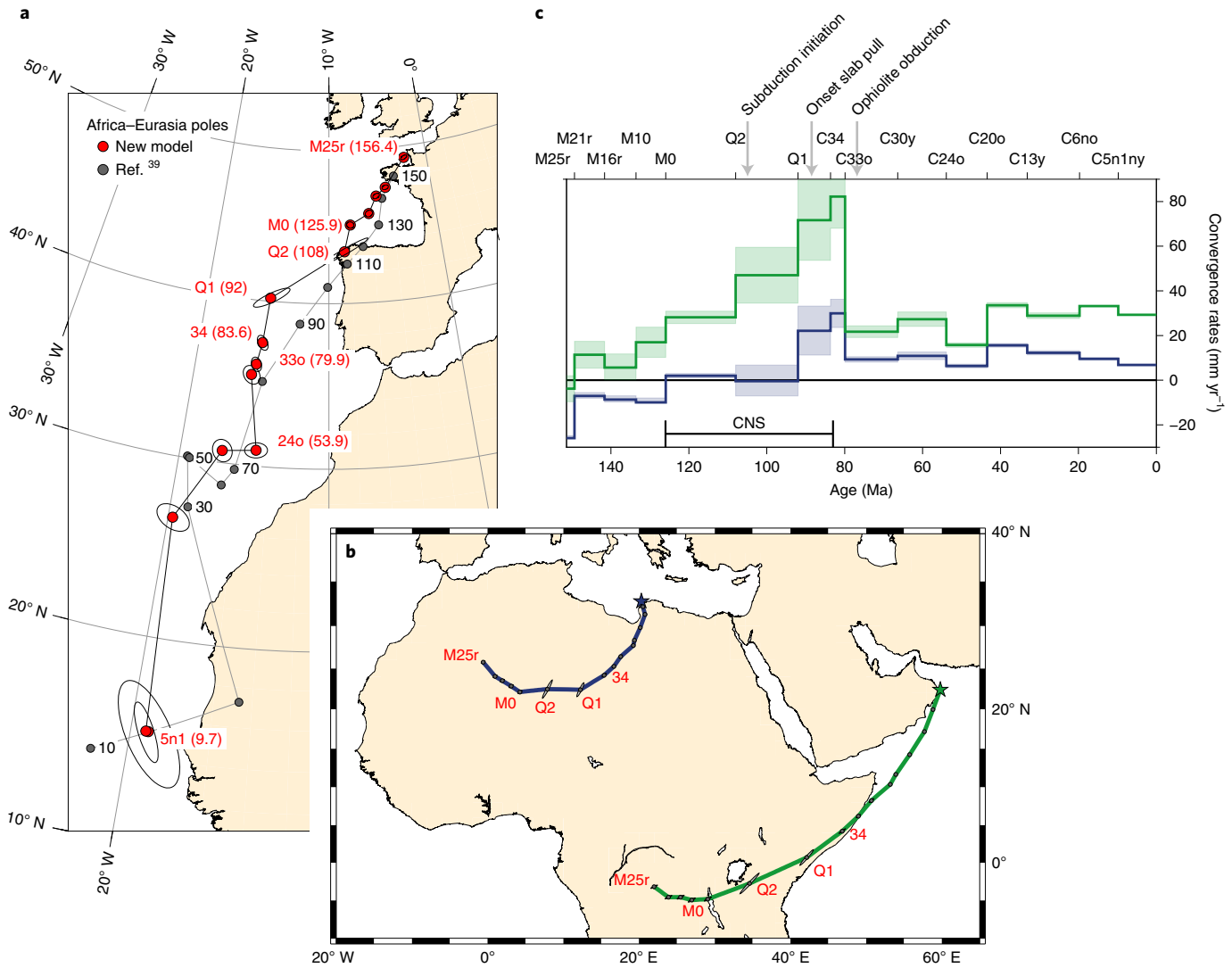

Fig. 3 | Africa–Eurasia relative plate motions since the Mesozoic. a, Location of Africa–Eurasia finite rotation poles (red circles) with 95% confidence ellipses. **b**, Predicted plate motion trajectories for the African Plate relative to the Eurasian Plate calculated on the basis of our revised kinematic model. The western trajectory (blue line) is based on Africa–Eurasia pole parameters whereas the eastern (green line) trajectory also includes the Neogene Arabia–Africa motion (Methods). Grey filled ellipses delineate the 95% confidence locations. **c**, Convergence rates computed along the synthetic trajectories. Shadings show the 1σ uncertainties. Convergence rates along with plate velocities are shown in Extended Data Fig. 4. Grey arrows indicate tectonic events.

passive margin[26,31] (Fig.1b). The rise of the Morondava mantle plume below the southwest Indian Ocean was identified as the likely trigger: plume rise induced radial plume-head spreading that triggered separation of India and Madagascar, whereby the cratonic keels of India and Africa acted as pivots around which the two plates underwent an opposite rotation causing east–west convergence in the Neotethys[11]. This convergence triggered subduction initiation parallel to the stepped continental margin of west India, Arabia and Greater Adria[11,22,26,31]. Seismic tomographic images show that even though the convergence driving subduction initiation was highly oblique to the Arabian–Greater Adriatic margin, it led to a slab, now located in the mid-mantle below Arabia and the eastern Mediterranean region, that is broadly parallel to the Cretaceous south Neotethyan margin[32]. Along the African–Arabian margin, the intra-oceanic subduction zone—and hence the associated slab pull—ceased between the ~85 Ma first arrival of African/Arabian continental crust in the trench and cessation of ophiolite obduction by ~70 Ma (refs. [22,33]) (Fig. 1c).

To evaluate whether the inception of slab pull in the new subduction zone may have been a trigger for a subsequent plate motion change, we explore numerical models of subduction dynamics. The geometry of the double, in-line subduction-zone configuration between Africa and Eurasia (Fig. 1b), which bears similarities to the Philippine Sea Plate today, has recently received considerable attention in the numerical modelling community, which predicted that the onset and arrest of double slab pull will generate pronounced plate accelerations and decelerations, respectively[12,34–37]. Convergence rates across coupled double subduction systems are predicted to be much faster than across a single subduction zone because of the pronounced slab pull exerted by two slabs working in tandem. Numerical models suggest that this stronger pull occurs because plates are not decoupled, but appear to 'communicate' through the dynamic pressure build-up in the mantle between them[34]. Numerical models of double, in-line subduction[12,34–37] thus predict acceleration of Africa–Eurasia convergence rates ~96–92 Ma due to onset of double slab pull and a deceleration sometime

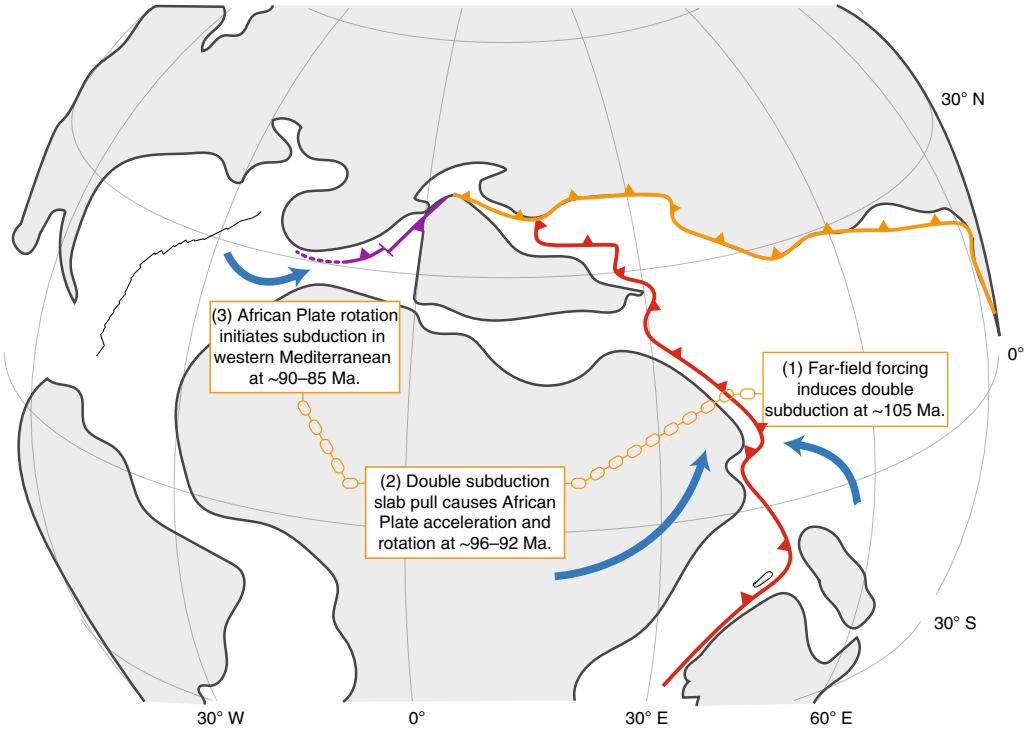

Fig. 4 | The chain of tectonic events in the Neotethys. African–Eurasia plate motion changes as the dynamic response to (1) plume-induced subduction initiation at ~105 Ma, followed by (2) the ~96–92 Ma onset of African Plate acceleration and rotation caused by double in-line slab pull along with forearc spreading, leading to (3) subduction initiation in the western Mediterranean at ~90–85 Ma and, finally, ~85–70 Ma arrest of double, in-line slab pull.

between ~85 and 70 Ma due to subduction arrest along the Arabian margin. To test that prediction, however, we first need to overcome the crude temporal resolution of the existing Africa–Eurasia plate kinematic models that stems from the lack of geomagnetic field reversals during the CNS.

Revised Africa–Eurasia plate kinematic model

Past Africa–Eurasia relative plate motions are calculated from restoring the opening of the Central and North Atlantic oceans through the Africa–North America–Eurasia plate circuit (Figs. 1 and 2). Previous reconstructions[38,39], without any kinematic constraints within the CQZ and without quantified uncertainties, proposed that Africa moved eastward with respect to Eurasia during the Early Cretaceous and later rotated northwards, sometime during the Cretaceous. These studies also suggested that Africa–Eurasia convergence rates since the Mesozoic have mostly been stable and small (<20 mm yr^{-1}). Importantly, the lack of geomagnetic polarity reversals between ~126 and 83.6 Ma (ref. [20]) (CNS, see Methods for discussion of the timescale) provides a major challenge for identifying the timing of the major anticlockwise rotation of Africa relative to Eurasia and its consequences on the evolution of convergence rates.

We present a revised Africa–Eurasia plate kinematic model that consists of rotation parameters (pole locations, angles of rotation and their uncertainties) for 15 time steps (magnetic anomalies) between 156 and 10 Ma, all of which are based on restoring conjugate sets of marine magnetic anomalies and fracture-zone crossings. We compute Africa–Eurasia motion by summing the rotation parameters of Africa–North America and North America–Eurasia (Methods, Fig. 3 and Extended Data Tables 1 and 2). Next, we overcome the challenge of the lack of polarity reversals during the CNS by tracing two magnetic anomaly features (Q1 and Q2[21]) that result from prominent changes in the behaviour of the geomagnetic field (Fig. 2 and Extended Data Fig. 1). Their ages were inferred in the Central Atlantic CQZs by drill-hole data and tectonic constraints at ~92 (Q1) and ~108 (Q2) Ma (ref. [21]). Together with independent seafloor fabric constraints as well as fracture-zone crossings, we computed intra-CNS finite rotation parameters for Africa–North America motion for Q1 and Q2 and combined them with the North America–Eurasia rotations. The transition from continental rifting to seafloor spreading between North America and Eurasia occurred during the CNS[40], and we cannot confidently identify Q1 or Q2 there. Our analysis assumes that during the CNS, the North America–Eurasia motion, as indicated by drill-hole data and the relatively simple North Atlantic fracture-zone orientations, was ultraslow and stable compared with the motion of Africa relative to North America[41] and combines the Africa–North America motion with the North America–Eurasia-interpolated rotation parameters for this period (Methods and Extended Data Figs. 2 and 3). We note that due to the ultraslow North America–Eurasia spreading rates, this assumption has minor effects on the resultant CNS Africa–Eurasia motions and associated uncertainties.

The resulting kinematic model (Fig. 3) implies that Africa convergence rates at the easternmost side of the plate boundary accelerated from low rates of ~20–30 mm yr^{-1} before the CNS and until Q2 to ~45 mm yr^{-1} averaged over the Q2–Q1 interval (108–92 Ma), followed by a spike at ~70–80 mm yr^{-1} between the Q1 and C33o (92–79.9 Ma) interval. The magnitude of plate acceleration decreases westwards, illustrating that the acceleration coincided with the anticlockwise rotation of Africa versus Eurasia (Fig. 3b,c). We note that the spike in convergence rate continued for a brief interval after the CNS (anomalies C34–C33o; 83.6–79.9 Ma), independently supporting the intra-CNS results. The spike was followed by a sharp deceleration at ~80 Ma, after which the convergence rates (Fig. 3c) and the relative plate directions (Fig. 3b) remained relatively stable.

Cretaceous plate tectonic chain reaction

Our plate kinematic constraints are consistent with numerical model predictions for plate kinematic response to double subduction-zone

inception and arrest[12,34–37]. It is thus feasible that the acceleration of Africa–Eurasia convergence, and the associated and synchronous anticlockwise rotation of Africa, is the dynamic response to the ~96–92 Ma onset of double slab pull, although the slight eastward component of slab pull may have led to a subtly smaller effect than predicted by the numerical experiments. The double slab pull affected only the eastern half of the African Plate, and the anticlockwise rotation of Africa is thus a logical response. The interpretation that plate motion change is the result of double slab pull is further supported by the coincidence of arrest of the intra-Neotethyan subduction zone between 85 and 70 Ma (refs. [22,33]) (Fig. 1c) and the sharp decrease in convergence rates that we observe (Fig. 3c). This shows that the intra-Neotethyan subduction zone that was induced from 104 Ma onwards by a plume-induced clockwise rotation of Africa versus India[11] became itself the driver of the next plate motion change on inception of slab pull.

Interestingly, the CNS anticlockwise rotation of Africa relative to Eurasia that we interpret as driven by the inception of slab pull (Fig. 3) induced convergence on a former transform fault in the western Mediterranean region. Before the rotation, Africa–Iberia and Africa–southern Europe motion was accommodated primarily along transform faults, but Africa–Eurasia anticlockwise change in rotation induced slow convergence that sparked two subduction zones with opposite polarities, straddling from Iberia to the western Alps[22] (Fig. 1). The oldest high-pressure metamorphic rocks associated with these new subduction zones, on Corsica[42] and in the western Alps[43], confirm that subduction was under way by ~85 Ma. Because convergence rates associated with this subduction were slow (<10 mm yr^{-1}, Fig. 3) and much of the subducting lithosphere in the Alps was continental[22], the inception of pronounced slab pull was long delayed. For the northwest-dipping slab below Iberia (Fig. 4), roll-back finally led to the opening of a back-arc basin across the western Mediterranean region from ~30 Ma onwards[44]. Roll-back rates of the south-dipping slab in the western Alps never exceeded African Plate advance, and both slabs were very narrow compared with the plates they were attached to. Thus, the dynamic changes they induced probably did not cause pronounced changes in Africa–Eurasia convergence but were restricted to western Mediterranean back-arc basin opening[44]. Nonetheless, the chain reaction will probably continue: arrival of the North African lithosphere in the western Mediterranean trench led to subduction arrest some 15 Ma[22], and ongoing Africa–Europe convergence is in the process of causing a reversal of subduction polarity, with Eurasian oceanic lithosphere starting to subduct below North Africa[45]. Inception of slab pull may at some stage in the future drive the next dynamic response.

Through combining dynamic causes and effects predicted by physics-based modelling with geologically documented kinematic evolution, we show that plate motion and plate boundary change induced by one trigger may become the driver of a subsequent plate reorganization event. Such plate tectonic chain reactions thus allow for long-term propagation of plate tectonic changes through a plate circuit and provide an avenue towards a dynamic underpinning of intriguing yet hitherto enigmatic global plate reorganizations. The plate tectonic chain reaction that we identify here propagated from a plate reorganization induced by mantle plume rise in the southwest Indian ocean to active subduction initiation in the western Mediterranean region over a period of ~100 Myr (Fig. 4). We foresee that, on the one hand, global plate reorganizations[5] may in fact be particularly rapid (that is, within a few million years) plate tectonic chain reactions initiated by a single trigger[5,7] that sets off a cascade of geodynamic events propagating through the global plate circuit. On the other hand, they may be a mere coincidence of several regional chain reactions responding to multiple unrelated triggers. Our analysis illustrates how the global plate circuit may be tied into a self-perpetuating chain of events and paves the way towards a mechanistic understanding of regional and global plate reorganizations.

Online content

Any methods, additional references, Nature Research reporting summaries, source data, extended data, supplementary information, acknowledgements, peer review information; details of author contributions and competing interests; and statements of data and code availability are available at https://doi.org/10.1038/s41561-022-00893-7.

Received: 13 May 2020; Accepted: 23 December 2021;
Published online: 03 March 2022

References

1. Torsvik, T. H., Müller, R. D., Van der Voo, R., Steinberger, B. & Gaina, C. Global plate motion frames: toward a unified model. *Rev. Geophys.* **46**, RG3004 (2008).
2. Matthews, K. J., Seton, M. & Müller, R. D. A global-scale plate reorganization event at 105–100 Ma. *Earth Planet. Sci. Lett.* **355–356**, 283–298 (2012).
3. Müller, R. D. et al. Ocean basin evolution and global-scale plate reorganization events since Pangea breakup. *Annu. Rev. Earth Planet. Sci.* **44**, 107–138 (2016).
4. Olierook, H. K. H. et al. Timing and causes of the mid-Cretaceous global plate reorganization event. *Earth Planet. Sci. Lett.* **534**, 116071 (2020).
5. Rona, P. A. & Richardson, E. S. Early Cenozoic global plate reorganization. *Earth Planet. Sci. Lett.* **40**, 1–11 (1978).
6. O'Connor, J. M. et al. Constraints on past plate and mantle motion from new ages for the Hawaiian–Emperor Seamount chain. *Geochem. Geophys. Geosyst.* **14**, 4564–4584 (2013).
7. Seton, M. et al. Ridge subduction sparked reorganization of the Pacific plate–mantle system 60–50 million years ago: Pacific plate–mantle reorganization. *Geophys. Res. Lett.* **42**, 1732–1740 (2015).
8. Whittaker, J. M. et al. Major Australian–Antarctic plate reorganization at Hawaiian–Emperor bend time. *Science* **318**, 83–86 (2007).
9. Cande, S. C. & Stegman, D. R. Indian and African plate motions driven by the push force of the Reunion plume head. *Nature* **475**, 47–52 (2011).
10. van Hinsbergen, D. J., Steinberger, B., Doubrovine, P. V. & Gassmöller, R. Acceleration and deceleration of India–Asia convergence since the Cretaceous: roles of mantle plumes and continental collision. *J. Geophys. Res. Solid Earth* **116**, B06101 (2011).
11. van Hinsbergen, D. J. et al. A record of plume-induced plate rotation triggering seafloor spreading and subduction initiation. *Nat. Geosci.* **14**, 626–630 (2021).
12. Jagoutz, O., Royden, L., Holt, A. F. & Becker, T. W. Anomalously fast convergence of India and Eurasia caused by double subduction. *Nat. Geosci.* **8**, 475–478 (2015).
13. Faccenna, C., Becker, T. W., Lallemand, S. & Steinberger, B. On the role of slab pull in the Cenozoic motion of the Pacific Plate. *Geophys. Res. Lett.* **39**, L03305 (2012).
14. Domeier, M. et al. Intraoceanic subduction spanned the Pacific in the Late Cretaceous–Paleocene. *Sci. Adv.* **3**, eaao2303 (2017).
15. Buiter, S. J. & Torsvik, T. H. A review of Wilson cycle plate margins: a role for mantle plumes in continental break-up along sutures? *Gondwana Res.* **26**, 627–653 (2014).
16. Stern, R. J. Subduction initiation: spontaneous and induced. *Earth Planet. Sci. Lett.* **226**, 275–292 (2004).
17. Wu, J. T.-J. & Wu, J. Izanagi–Pacific ridge subduction revealed by a 56 to 46 Ma magmatic gap along the northeast Asian margin. *Geology* **47**, 953–957 (2019).
18. Guilmette, C. et al. Forced subduction initiation recorded in the sole and crust of the Semail Ophiolite of Oman. *Nat. Geosci.* **11**, 688–695 (2018).
19. Agard, P., Jolivet, L., Vrielynck, B., Burov, E. & Monie, P. Plate acceleration: the obduction trigger? *Earth Planet. Sci. Lett.* **258**, 428–441 (2007).
20. Ogg, J. G. in *The Geologic Time Scale 2012* (eds Gradstein, F. M. et al.) 85–114 (Elsevier, 2012).
21. Granot, R., Dyment, J. & Gallet, Y. Geomagnetic field variability during the Cretaceous Normal Superchron. *Nat. Geosci.* **5**, 220–223 (2012).
22. van Hinsbergen, D. J. J. et al. Orogenic architecture of the Mediterranean region and kinematic reconstruction of its tectonic evolution since the Triassic. *Gondwana Res.* **81**, 79–229 (2020).
23. Gürer, D., van Hinsbergen, D. J. J., Matenco, L., Corfu, F. & Cascella, A. Kinematics of a former oceanic plate of the Neotethys revealed by deformation in the Ulukışla basin (Turkey). *Tectonics* **35**, 2385–2416 (2016).

24. Rioux, M. et al. Tectonic development of the Samail ophiolite: high-precision U–Pb zircon geochronology and Sm–Nd isotopic constraints on crustal growth and emplacement. *J. Geophys. Res.* **118**, 2085–2101 (2013).
25. Parlak, O. The Tauride ophiolites of Anatolia (Turkey): a review. *J. Earth Sci.* **27**, 901–934 (2016).
26. van Hinsbergen, D. J. J., Maffione, M., Koornneef, L. M. & Guilmette, C. Kinematic and paleomagnetic restoration of the Semail ophiolite (Oman) reveals subduction initiation along an ancient Neotethyan fracture zone. *Earth Planet. Sci. Lett.* **518**, 183–196 (2019).
27. Gaina, C. & Jakob, J. Global Eocene tectonic unrest: possible causes and effects around the North American plate. *Tectonophysics* **760**, 136–151 (2019).
28. Schellart, W. P. Andean mountain building and magmatic arc migration driven by subduction-induced whole mantle flow. *Nat. Commun.* **8**, 2010 (2017).
29. Tavani, S., Corradetti, A., Sabbatino, M., Seers, T. & Mazzoli, S. Geological record of the transition from induced to self-sustained subduction in the Oman Mountains. *J. Geodyn.* **133**, 101674 (2020).
30. Pourteau, A. et al. Thermal evolution of an ancient subduction interface revealed by Lu–Hf garnet geochronology, Halilbağı Complex (Anatolia). *Geosci. Front.* **10**, 127–148 (2019).
31. Maffione, M., van Hinsbergen, D. J. J., de Gelder, G. I. N. O., van der Goes, F. C. & Morris, A. Kinematics of Late Cretaceous subduction initiation in the Neo-Tethys Ocean reconstructed from ophiolites of Turkey, Cyprus, and Syria. *J. Geophys. Res.* **122**, 3953–3976 (2017).
32. van der Meer, D. G., van Hinsbergen, D. J. J. & Spakman, W. Atlas of the underworld: slab remnants in the mantle, their sinking history, and a new outlook on lower mantle viscosity. *Tectonophysics* **723**, 309–448 (2018).
33. Warren, C. J., Parrish, R. R., Waters, D. J. & Searle, M. P. Dating the geologic history of Oman's Semail ophiolite: insights from U–Pb geochronology. *Contrib. Mineral. Petrol.* **150**, 403–422 (2005).
34. Holt, A. F., Royden, L. H. & Becker, T. W. The dynamics of double slab subduction. *Geophys. J. Int.* **209**, 250–265 (2017).
35. Čížková, H. & Bina, C. R. Geodynamics of trench advance: insights from a Philippine-Sea-style geometry. *Earth Planet. Sci. Lett.* **430**, 408–415 (2015).
36. Pusok, A. E. & Stegman, D. R. Formation and stability of same-dip double subduction systems. *J. Geophys. Res.* **124**, 7387–7412 (2019).
37. Király, Á., Funiciello, F., Capitanio, F. A. & Faccenna, C. Dynamic interactions between subduction zones. *Glob. Planet. Change* **202**, 103501 (2021).
38. Dewey, J. F., Helman, M. L., Knott, S. D., Turco, E. & Hutton, D. H. W. Kinematics of the western Mediterranean. *Geol. Soc. Lond. Spec. Publ.* **45**, 265–283 (1989).
39. Rosenbaum, G., Lister, G. S. & Duboz, C. Relative motions of Africa, Iberia and Europe during Alpine orogeny. *Tectonophysics* **359**, 117–129 (2002).
40. Péron-Pinvidic, G., Manatschal, G., Minshull, T. A. & Sawyer, D. S. Tectonosedimentary evolution of the deep Iberia–Newfoundland margins: evidence for a complex breakup history. *Tectonics* **26**, TC2011 (2007).
41. Merkouriev, S. & DeMets, C. A high-resolution model for Eurasia–North America plate kinematics since 20 Ma. *Geophys. J. Int.* **173**, 1064–1083 (2008).
42. Lahondère, D. & Guerrot, C. Datation Sm-Nd du métamorphisme éclogitique en Corse alpine: un argument pour l'existence au Crétacé supérieur d'une zone de subduction active localisée sous le bloc corso-sarde. *Geol. Fr.* **3**, 3–11 (1997).
43. Manzotti, P., Ballèvre, M., Zucali, M., Robyr, M. & Engi, M. The tectonometamorphic evolution of the Sesia–Dent Blanche nappes (internal Western Alps): review and synthesis. *Swiss J. Geosci.* **107**, 309–336 (2014).
44. Chertova, M. V., Spakman, W., Geenen, T., van den Berg, A. P. & van Hinsbergen, D. J. J. Underpinning tectonic reconstructions of the western Mediterranean region with dynamic slab evolution from 3-D numerical modeling. *J. Geophys. Res.* **119**, 5876–5902 (2014).
45. Hamai, L. et al. Towards subduction inception along the inverted North African margin of Algeria? Insights from thermo-mechanical models. *Earth Planet. Sci. Lett.* **501**, 13–23 (2018).
46. van der Meer, D. G., Spakman, W., van Hinsbergen, D. J. J., Amaru, M. L. & Torsvik, T. H. Towards absolute plate motions constrained by lower-mantle slab remnants. *Nat. Geosci.* **3**, 36–40 (2010).
47. Sandwell, D. T., Müller, R. D., Smith, W. H. F., Garcia, E. & Francis, R. New global marine gravity model from CryoSat-2 and Jason-1 reveals buried tectonic structure. *Science* **346**, 65–67 (2014).

Methods

Timescale. We adopt the timescale of ref. [20] because it intercalibrated, among others, bio- and magnetostratigraphy. The onset of the CNS (anomaly M0) in that timescale is assigned the age of ~126 Ma, but this age is rather uncertain and the actual age may in fact be closer to ~121 Ma[4,48]. Because we compare geological events and reconstructions of the Neotethys, largely on the basis of biostratigraphic dating, with marine magnetic anomalies, our study requires an intercalibrated timescale, explaining our choice of the ref. [20] timescale. We note that shifting the age of the base of the CNS to ~121 Ma would have negligible effect on the convergence rates before Q1 (92 Ma) as the direction of Africa–Eurasia relative plate motion nearly paralleled the margin at that time. The ages of Q1 and Q2 were supported by dated oldest sediments from the ocean floor close to these anomalies (DSDP sites 137 and 386, Fig. 2) and a seafloor spreading model between anomalies M0 and C34[21] and are thus only slightly (to within ~1 Myr) affected by the age of the base of the CNS.

Neotethys reconstruction. The palaeotectonic map at 92 Ma shown in Fig. 1 is based on a systematic kinematic restoration of plate motions, orogenic deformation and palaeomagnetically constrained rotations. Restoration of orogens in the Mediterranean region[22,23,31], Iran[49] and Oman[26] are based on quantitative structural geological constraints on reconstruction of back-arc extension, transform motion, shortening and palaeomagnetic data, in that order. The amount of shortening associated with stacking of orogenic nappes, and the reconstructed palaeogeographic width of the platforms and basins from which these nappes were derived, is based on the amount of plate convergence constrained from the plate circuit that occurred during the underthrusting of the nappes as constrained by stratigraphic, metamorphic and sedimentological data, whereby the amount of geologically documented shortening is used as a minimum value[22,44]. Reconstructions are tested against and iteratively improved using palaeomagnetic constraints on vertical axis rotations while obeying structural geological data. Intra-oceanic plate motion and original intra-oceanic trench motion are constrained from palaeomagnetic data on palaeolatitude and palaeodyke orientations preserved in supra-subduction-zone ophiolites of Anatolia, Cyprus, Syria and Oman[26,31,50]. Initiation of intra-oceanic subduction from Oman to Turkey is constrained by Lu/Hf garnet crystallization ages of the metamorphic soles of ophiolites of Oman and Anatolia that consistently reveal ages of ~104 Ma (refs. [18,30]). Initiation of supra-subduction-zone spreading in the forearc of the intra-Tethyan subduction zone follows from zircon U/Pb ages from gabbros and plagiogranites preserved as ophiolites, showing ages of ~96–95 Ma for Oman[24] and ~92–90 Ma for Anatolia and Cyprus[25,50]. Predicted locations of subducted slabs at the moment of their break-off, rotated in a mantle reference frame[51], are consistent with the locations of subducted slabs in the underlying mantle constrained from seismic tomography[32,52].

The kinematic model of Neotethyan intra-oceanic subduction was made in GPlates plate reconstruction software[53] using the work flow detailed in ref. [11]. For the Central Atlantic CQZ, we computed CNS rotation pole parameters on the basis of magnetic anomaly and fracture-zone picks.

Africa–North America plate motion. We employed and adopted the results of kinematic investigations that used a best-fitting criteria[54] and statistical approach[55] to compute the rotation parameters and their uncertainties for a set of plate pairs. For the post-CNS period, we adopted the North America–Africa kinematic solutions of refs. [56,57]. The available Mesozoic kinematic solutions lack uncertainties; therefore, we re-computed the M0, M10, M16r, M21r and M25r finite rotation parameters using the magnetic picks of refs. [58,59], for which we added fracture-zone crossings based on satellite gravity data[47]. We also computed two internal rotation parameters for the Cretaceous Normal Superchron on the basis of identification of magnetic anomalies (Q1 and Q2, Fig. 1 and Extended Data Fig. 1) that have arisen due to prominent changes in the behaviour of the geomagnetic field[21]. These features were used to compute the plate kinematics for the Cretaceous South Atlantic Ocean (Africa–South America plates[60]) and resulted in opening ages of the equatorial Atlantic that are consistent with global isotopic signatures of benthic foraminifera[55]. We here follow a similar approach and internally date the Central Atlantic CQZs by tracing these two magnetic features on the basis of the available sea surface marine magnetic data (Extended Data Fig. 1). Satellite-derived gravity grids now have sufficient accuracy to trace seafloor fabric (abyssal hills[47]), which provides additional independent constraint on the orientation of the isochrons. The implemented Q1 and Q2 Africa–North America kinematic solutions, with their 95% uncertainty intervals, are shown in Extended Data Fig. 2 and Extended Data Table 2. Most of the values of the statistical parameter ($\hat{\kappa}$) are near one (Extended Data Table 2), indicating that the uncertainty assigned to the data points (magnetic and fracture-zone picks were assigned 4 and 5 km, respectively) used to calculate the solutions were reasonable[55]. For anomaly Q2, the value of $\hat{\kappa}$ is 5.5, indicating that the error values for the picks were overestimated by a factor of 2.3. We note that rescaling the error estimates would make only a minor difference in the size of the uncertainty ellipse.

North America–Eurasia plate motion. We adopted the Eurasia–North America Cenozoic kinematic solutions of refs. [41,61]. The implemented Q1 and Q2 Africa–Eurasia kinematic solutions, with their 95% uncertainty intervals, are shown in Extended Data Fig. 3. The solution for C30y was interpolated using C25y and C31y solutions. The complex transition from continental rifting to ultraslow seafloor spreading that occurred during the CNS prevent us from confidently recognizing the internal quiet zone anomalies. We thus adopted the M25 rotation pole of ref. [62] of which the location is based on seafloor data of the oldest magnetic anomaly and the angle was extended to bring the palaeomagnetic poles of Eurasia and North America to fit. The rotation parameters of M21r, M16r, M10, M0, Q2 and Q1 were interpolated using C34 and M25 kinematic solutions[61–63]. Since very slow extensional rates prevailed at this pre-seafloor-spreading stage, the locations of the interpolated Mesozoic poles (and their uncertainties) have negligible effect on the resultant Africa–Eurasia finite rotation poles.

Africa–North America–Eurasia plate circuit. Mesozoic and Cenozoic motions of the African Plate relative to the Eurasia Plate were calculated through the Africa–North America–Eurasia plate circuit. Finite rotations, and their uncertainties, were combined[64] (Fig. 3 and Extended Data Table 2), giving temporal resolution of ~10 Myr throughout the studied period (the past 156 Myr). The easternmost part of Africa is now located on the Arabian Plate; thus, to calculate the trajectories and relative velocities of the area that is now part of Arabia, we added published Arabian–African rotation poles[56].

Data availability

Rotation and shape files for plate kinematic model made in GPlates reconstruction software[53] were provided as supplementary information to previous papers[22,26,49,65]. GPlates files with reconstructions used to draft Figs. 1 and 4 are provided at https://figshare.com/articles/dataset/van_Hinsbergen_NatureGeo_2021_GPlates_zip/13516727. Marine magnetic data can be obtained at the NCEI GEODAS database: https://www.ngdc.noaa.gov/mgg/geodas/trackline.html.

Code availability

GPlates plate reconstruction software[53] used for developing our plate kinematic model is available from https://www.gplates.org/.

References

48. Midtkandal, I. et al. The Aptian (Early Cretaceous) oceanic anoxic event (OAE1a) in Svalbard, Barents Sea, and the absolute age of the Barremian–Aptian boundary. *Palaeogeogr. Palaeoclimatol. Palaeoecol.* **463**, 126–135 (2016).
49. McQuarrie, N. & van Hinsbergen, D. J. J. Retrodeforming the Arabia–Eurasia collision zone: age of collision versus magnitude of continental subduction. *Geology* **41**, 315–318 (2013).
50. van Hinsbergen, D. J. J. et al. Tectonic evolution and paleogeography of the Kırşehir Block and the Central Anatolian ophiolites, Turkey. *Tectonics* **35**, 983–1014 (2016).
51. Doubrovine, P. V., Steinberger, B. & Torsvik, T. H. Absolute plate motions in a reference frame defined by moving hot spots in the Pacific, Atlantic, and Indian oceans. *J. Geophys. Res.* **117**, B09101 (2012).
52. Gürer, M. D. *Subduction Evolution in the Anatolian Region: The Rise, Demise, and Fate of the Anadolu Plate*. PhD dissertation, Utrecht Univ. (2017).
53. Boyden, J. A. et al. in *Geoinformatics: Cyberinfrastructure for the Solid Earth Sciences* (eds Keller, G. R. & Baru, C.) 95–113 (Cambridge Univ. Press, 2011).
54. Hellinger, S. J. The uncertainties of finite rotations in plate tectonics. *J. Geophys. Res.* **86**, 9312–9318 (1981).
55. Royer, J.-Y. & Chang, T. Evidence for relative motions between the Indian and Australian plates during the last 20 m.y. from plate tectonic reconstructions: implications for the deformation of the Indo-Australian plate. *J. Geophys. Res.* **96**, 11779–11802 (1991).
56. Merkouriev, S. & DeMets, C. High-resolution estimates of Nubia–North America plate motion: 20 Ma to present. *Geophys. J. Int.* **196**, 1281–1298 (2013).
57. Müller, R. D., Royer, J.-Y., Cande, S. C., Roest, W. R. & Maschenkov, S. in *Sedimentary Basins of the World* Vol. 4 (ed. Mann, P.) 33–59 (Elsevier, 1999).
58. Klitgord, K. D. & Schouten, H. in *The Western North Atlantic Region* (eds Vogt, P. R. & Tucholke, B. E.) 351–378 (GSA, 1986); https://doi.org/10.1130/DNAG-GNA-M.351
59. Seton, M. et al. Community infrastructure and repository for marine magnetic identifications. *Geochem. Geophys. Geosyst.* **15**, 1629–1641 (2014).
60. Granot, R. & Dyment, J. The Cretaceous opening of the South Atlantic Ocean. *Earth Planet. Sci. Lett.* **414**, 156–163 (2015).
61. Gaina, C., Roest, W. R. & Müller, R. D. Late Cretaceous–Cenozoic deformation of northeast Asia. *Earth Planet. Sci. Lett.* **197**, 273–286 (2002).
62. Torsvik, T. H., Van der Voo, R., Meert, J. G., Mosar, J. & Walderhaug, H. J. Reconstructions of the continents around the North Atlantic at about the 60th parallel. *Earth Planet. Sci. Lett.* **187**, 55–69 (2001).

63. Doubrovine, P. V. & Tarduno, J. A. A revised kinematic model for the relative motion between Pacific oceanic plates and North America since the Late Cretaceous. *J. Geophys. Res.* **113**, B12101 (2008).
64. Chang, T., Stock, J. & Molnar, P. The rotation group in plate tectonics and the representation of uncertainties of plate reconstructions. *Geophys. J. Int.* **101**, 649–661 (1990).
65. Gürer, D. & van Hinsbergen, D. J. J. Diachronous demise of the Neotethys Ocean as a driver for non-cylindrical orogenesis in Anatolia. *Tectonophysics* **760**, 95–106 (2019).
66. Malinverno, A., Hildebrandt, J., Tominaga, M. & Channell, J. E. T. M-sequence geomagnetic polarity time scale (MHTC12) that steadies global spreading rates and incorporates astrochronology constraints. *J. Geophys. Res.* **117** (2012).

Acknowledgements

D.G. did not receive any specific funding for this work. R.G. acknowledges ISF grant 1923/21. D.J.J.v.H. acknowledges NWO Vici grant 865.17.001. The funders had no role in study design, data collection and analysis, decision to publish or preparation of the manuscript.

Author contributions

D.G., R.G. and D.J.J.v.H. contributed equally to the design of the research, the conduction of research and the writing of the paper.

Competing interests

The authors declare no competing interests.

Additional information

Extended data is available for this paper at https://doi.org/10.1038/s41561-022-00893-7.

Supplementary information The online version contains supplementary material available at https://doi.org/10.1038/s41561-022-00893-7.

Correspondence and requests for materials should be addressed to Derya Gürer.

Peer review information *Nature Geoscience* thanks Lucia Perez-Diaz and the other, anonymous, reviewer(s) for their contribution to the peer review of this work. Primary Handling Editors: Tamara Goldin; Stefan Lachowycz.

Reprints and permissions information is available at www.nature.com/reprints.

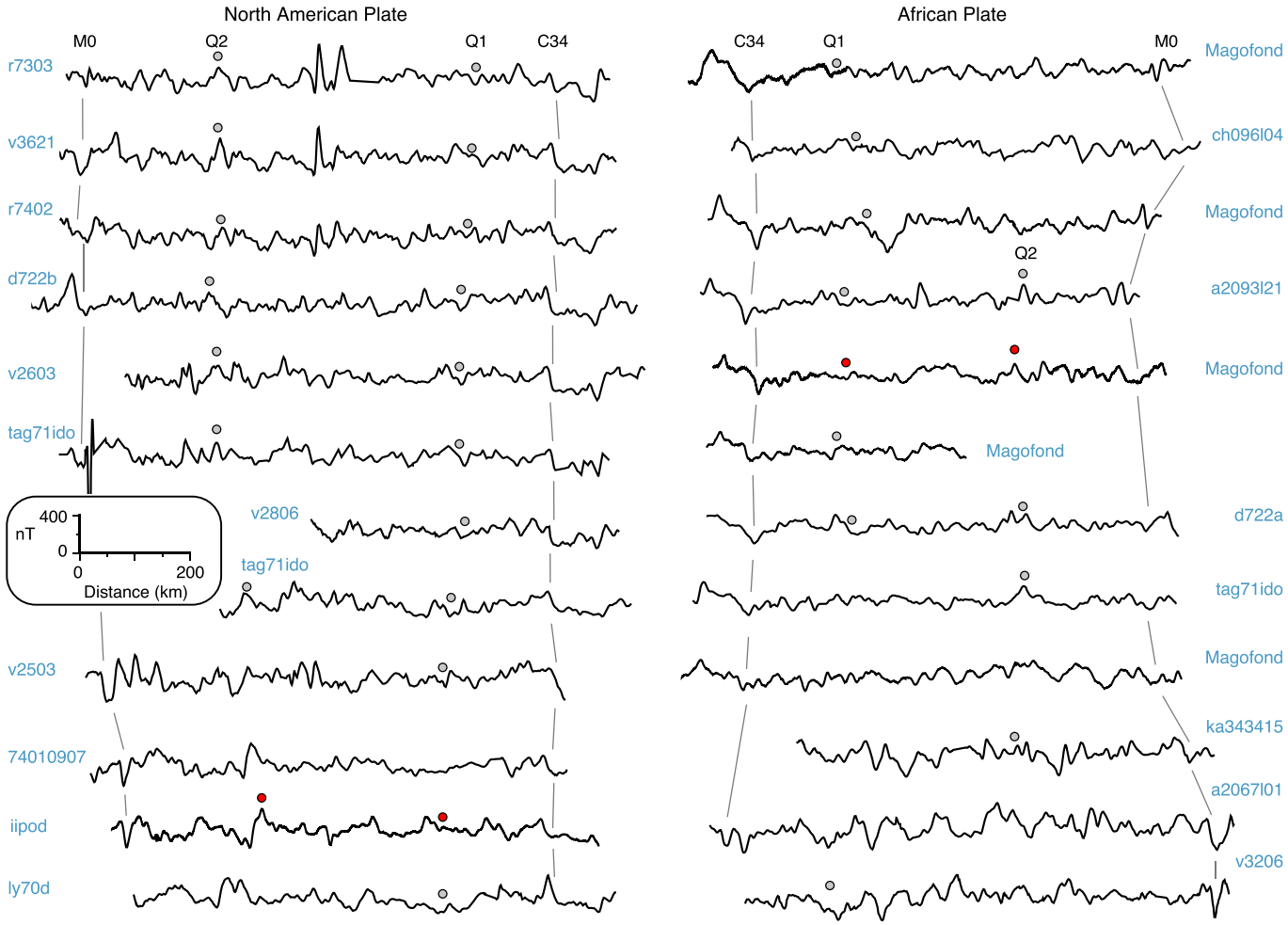

Extended Data Fig. 1 | Magnetic anomaly sea surface representative profiles used for the kinematic analysis of the Central Atlantic quiet zones. The observed magnetic profiles are ordered from north (top) to south (bottom). Magnetic identification of Q1 and Q2 are shown in two profiles with red circles[21]. These anomalies were then traced outward into the other Central Atlantic magnetic profiles[21] (gray circles), using both the magnetic anomalies backed by the vertical gradient of the gravity field (Fig. 1) that provide independent constraints on the crustal structure and seafloor fabric. Sources of data are the National Centers for Environmental Information (NCEI) and Ifremer databases.

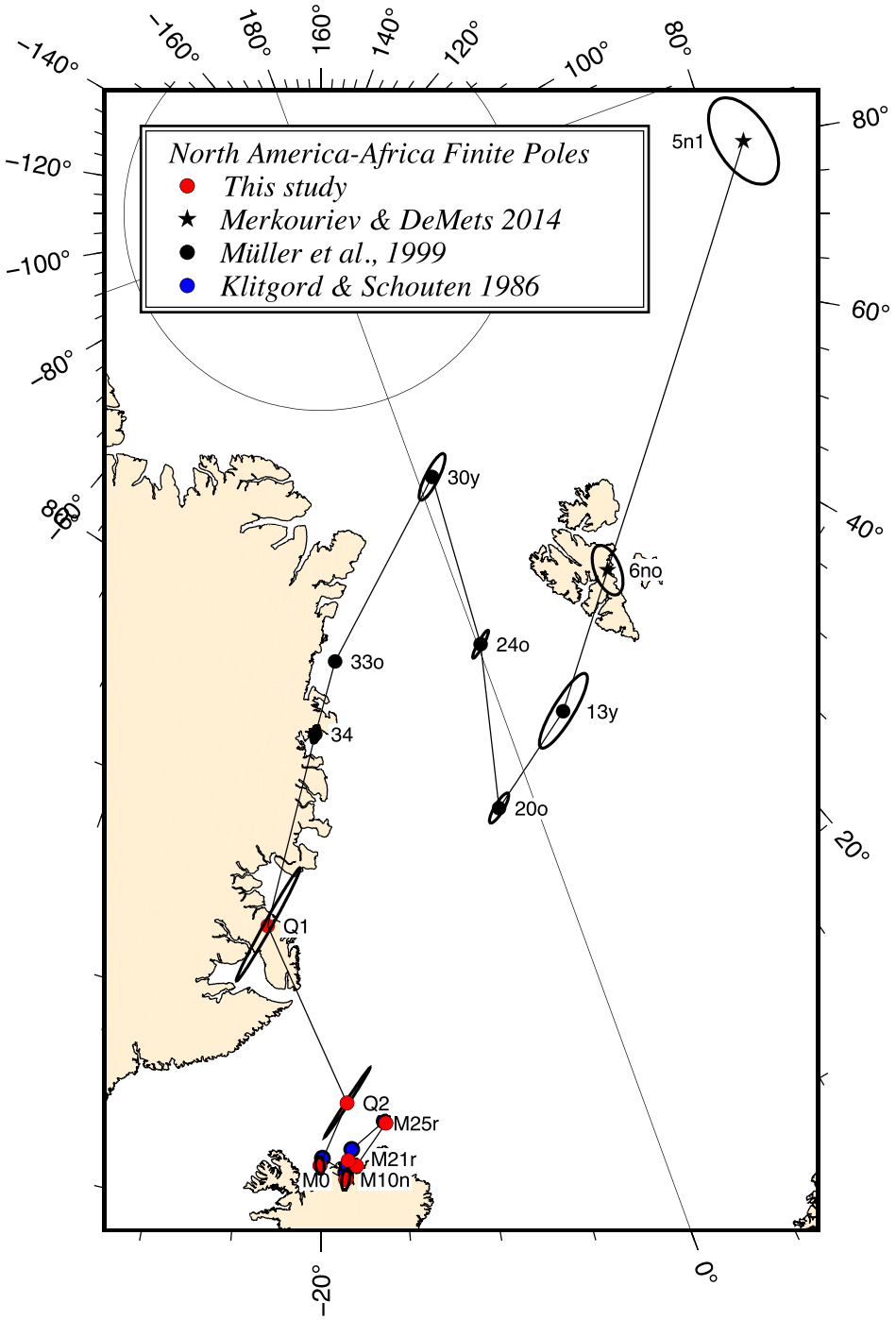

Extended Data Fig. 2 | North America–Africa finite rotation poles. North America-Africa finite rotation poles and their 95% confidence ellipses.

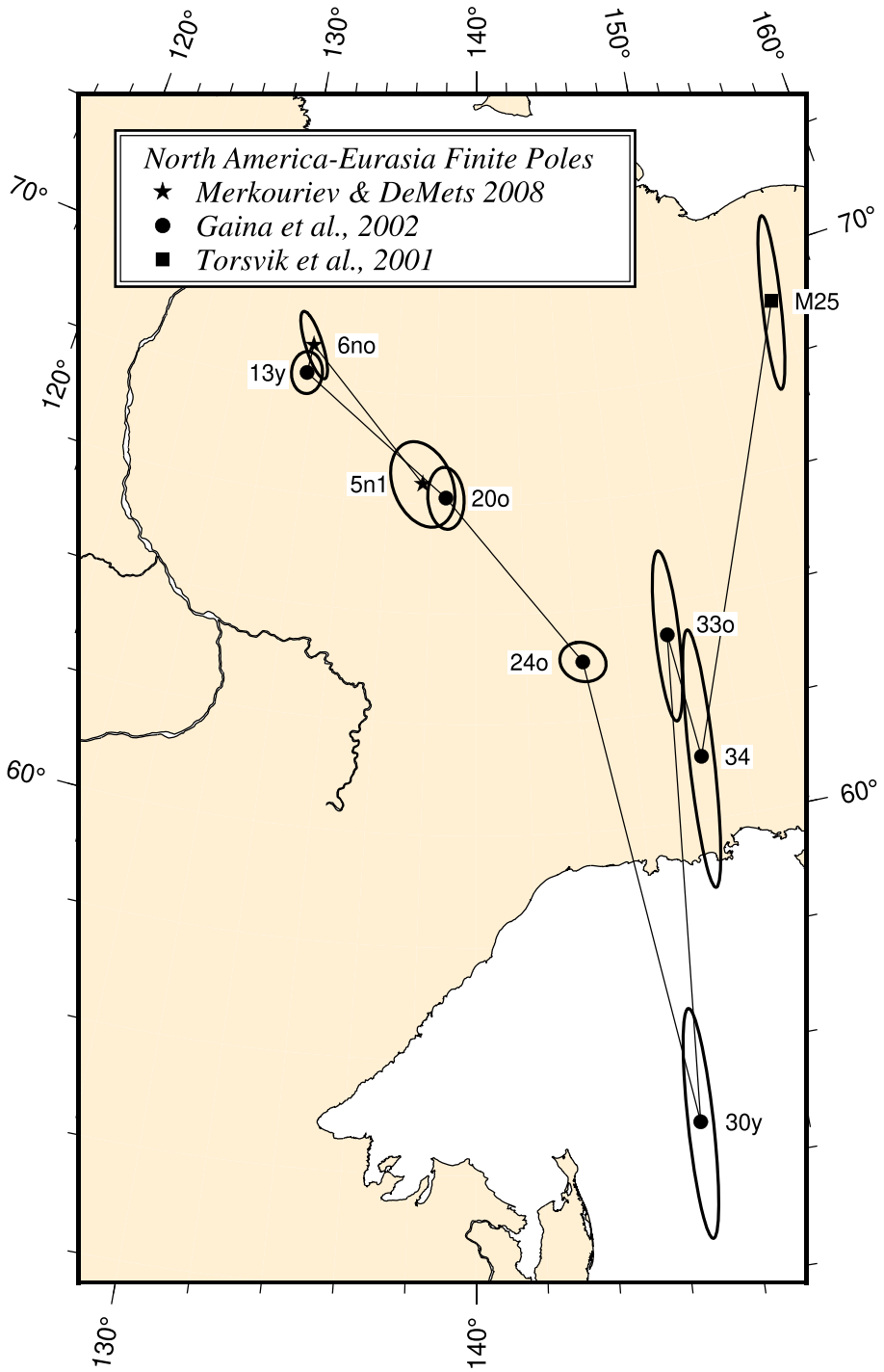

Extended Data Fig. 3 | North America–Eurasia finite rotation poles. North America- Eurasia finite rotation poles and their 95% confidence ellipses.

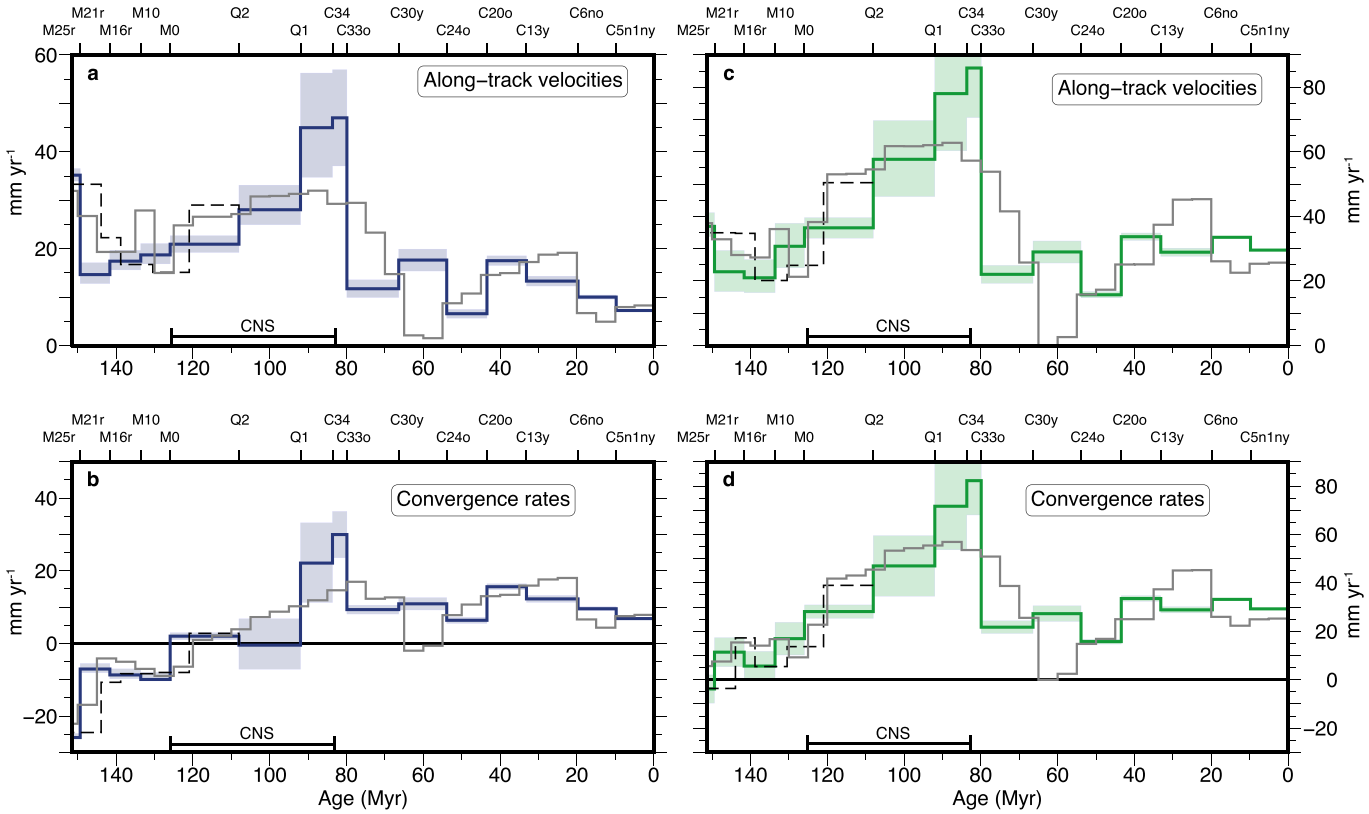

Extended Data Fig. 4 | Africa–Eurasia relative plate motions since the Mesozoic. Velocities along-track (**a**,**c**) and convergence rates (**b**,**d**) for the trajectories shown in Fig. 3b (a-b and c-d are calculated using the western and eastern trajectory, respectively). The velocities were calculated using the geomagnetic polarity time scale of Ogg[20]. Dashed lines delineate the Mesozoic rates when using the Malinverno et al.[66]. timescale. Grey lines show previous estimates of convergence rates inferred from interpolating plate motion change across the entire Cretaceous Normal Superchron[39]. Blue shadings show the 1σ uncertainties that were calculated based on the uncertainties of the reconstructed points. Convergence rates are the margin-orthogonal components of the relative motions, calculated along northward (**b**) or N30°E (**d**) direction.

Extended Data Table 1 | The source of the rotation parameters used in this study

Magnetic anomaly	Age [Ma]	North America - Africa	North America - Eurasia	Age source
C5n.1n (C5n.1y)	9.786	Merkouriev, 2014 (ref.[66])	Merkouriev, 2008 (ref.[41])	Ogg 2012 (ref.[3])
C6no	19.722	Merkouriev, 2014 (ref. [66])	Merkouriev, 2008 (ref. [41]	
C13n (C13y)	33.157	Müller 1999 (ref.[58])	Gaina 2002 (ref.[62])	
C20no (C20o)	43.43	Müller 1999 (ref.[58]) (interpolated)	Gaina 2002 (ref.[62])	
C24n.3no (C24o)	53.93	Müller 1999 (ref.[58]) (interpolated)	Gaina 2002 (ref.[62])	
C30n (C30y)	66.398	Müller 1999 (ref.[58])	Gaina 2002 (ref.[62]) (interpolated)	
C33o	79.9	Müller 1999 (ref.[58])	Gaina 2002 (ref.[62])	
C34n (C34)	83.64	Müller 1999 (ref.[58])	Gaina 2002 (ref.[62])	
Q1	92	This study	Interpolated	Granot 2012 (ref.[21])
Q2	108	This study	Interpolated	
M0	125.93 (120.95)	This study	Interpolated	Ogg 2012 (ref.[20]) Malinverno 2012 (ref.[67])
M10	133.58 (130.43)	This study	Interpolated	
M16r	141.64 (138.82)	This study	Interpolated	
M21r	149.35 (143.89)	This study	Interpolated	
M25r	156.42 (151.36)	This study	Torsvik 2001 (ref.[63])	

Extended Data Table 2 | Finite rotations and covariance matrices for the relative motion of Africa relative to North America (fixed)

Mag. Ano	Lat (°N)	Long (°E)	Angle (°)	$\hat{\kappa}$	a	b	c	d	e	f	g
Q1	71.98	-24.26	35.88	1.81	2.48	-4.05	2.71	6.69	-4.49	3.02	5
Q2	67.64	-18.30	46.76	5.56	3.70	-7.12	4.82	13.77	-9.33	6.34	5
M0	66.12	-20.05	54.41	0.78	10.52	-7.47	1.91	8.69	-4.65	3.87	7
M10	66.77	-18.52	57.58	0.50	9.90	-9.64	5.14	11.94	-7.27	5.15	7
M16r	66.23	-18.33	59.70	1.02	9.86	-11.08	5.37	15.25	-8.44	5.24	7
M21r	66.10	-17.85	62.12	2.15	13.90	-9.53	1.74	9.89	-4.12	3.07	7
M25r	67.10	-15.90	64.70	1.78	7.60	-6.31	1.39	8.77	-4.21	3.20	7

The covariance matrix is given by the formula $\frac{1}{\kappa} * \begin{pmatrix} a & b & c \\ b & d & e \\ c & e & f \end{pmatrix} \times 10^{-g}$ radians^2